Journal of Achievements in Materials and Manufacturing Engineering
VOLUME 37
ISSUE 1
November
2009

Structure and mechanical properties of PVD gradient coatings deposited onto tool steels and sialon tool ceramics

L.A. Dobrzański [a,*], M. Staszuk [a], A. Kříž [b], K. Lukaszkowicz [a]
[a] Division of Materials Processing Technology, Management and Computer Techniques in Materials Science, Institute of Engineering Materials and Biomaterials, Silesian University of Technology, ul. Konarskiego 18a, 44-100 Gliwice, Poland
[b] Faculty of Materials Science and Metallurgy, University of West Bohemia, Univerzitni 8, 306 14 Plzen, Czech Republic
* Corresponding author: E-mail address: leszek.dobrzanski@polsl.pl

Received 10.09.2009; published in revised form 01.11.2009

Properties

ABSTRACT

Purpose: The paper presents investigation results of the structure and mechanical properties of gradient coatings deposited by cathodic arc evaporation - physical vapour deposition (CAE-PVD) techniques onto the X40CrMoV5-1 hot work tool steel, HS6-5-2 high speed steel and SiAlON tool ceramics. The Ti(C,N), (Ti,Al)N and (Al,Si,Cr) N coatings were investigated.
Design/methodology/approach: Microstructure was characterised using scanning and transmission electron microscopy. The phase composition of the investigated coatings was determined by means of the X-ray diffractometer. The chemical concentration changes of the coating components, and the substrate material were evaluated in virtue of tests carried out in the GDOS spectrometer. Tests of the coatings' adhesion to the substrate material were made using the scratch test method.
Findings: It was found out that the structure of the PVD coatings deposited onto all substrates is composed of fine crystallites. The investigations made by use of the glow discharge optical emission spectrometer indicate to the existence of the transition zone between the substrate material and the coating. The results show that all coatings present good adhesion. The critical load L_{C2}, which is in the range 35-90 N, depends on the coating type and substrate. Good adhesion of the coatings deposited to the substrate should be connected with the existence of the transition zone. All the coatings are demonstrated by high hardness.
Research limitations/implications: Ti(C,N), (Ti,Al)N and (Al,Si,Cr) N gradient coatings can be applied for cutting tools and hot working tools.
Originality/value: Working out and testing PVD coatings obtained by tool ceramic and tool steels is a special future of development direction in a domain of thin coatings.
Keywords: Thin & thick coatings; Surface treatment; Mechanical properties

Reference to this paper should be given in the following way:
L.A. Dobrzański, M. Staszuk, A. Kříž, K. Lukaszkowicz, Structure and mechanical properties of PVD gradient coatings deposited onto tool steels and sialon tool ceramics, Journal of Achievements in Materials and Manufacturing Engineering 37/1 (2009) 36-43.

1. Introduction

Gradient coatings deposited on the tool material substrate and providing appropriately high resistance to abrasive wear in tool operating conditions, core ductility and stress relaxation between the particular coating layers and between the gradient coating and tool material coating are seen as a solution to the issue [1-8]. Functional gradient coatings create a new class of coatings with properties and structure changing gradually. Frequently a rapid difference between the coating and substrate properties occurs causing a stress concentration in this area, both during the manufacturing and operation of the tools. This causes fast degradation demonstrated by cracks and delamination of the coatings. The application of functional gradient coatings offers a possible solution of the issue. Gradient coatings can be applied for manufacturing modern machining tools, due to their resistance to high-temperature oxidation and erosion as well as abrasive wear.

Sialons were worked out at the end of the XX century. They create a new kind of sintering tool materials that are simultaneously connecting advantages of oxide and oxygen-free ceramics including Si_3N_4. Sialon is isomorphous with silicon nitride, when it is defined by a chemical formula $Si_{6-z}O_zN_{8-z}$, where atomic number Al replacing Si in a nitride lattice is equal *z* (z=0÷4.5). Mechanical and physical qualities of this phase are similar to each other, for the sake of similarity of crystallographic form of sialon to oxide nitride. However, mechanical qualities of sialon ceramics comply with oxide aluminium Al_2O_3. Sialons are used at cut point and applied for milling and turning cast iron, alloys on nickel base, steel after thermal treatment as well as titanium and aluminum alloys. Efficiency of machining using a *β'*-SiAlON cut points is significantly higher, than using other edges made of tool ceramics and sintered carbides [9-14].

The aim of this paper is to examine the structure and mechanical properties of the gradient coatings deposited by PVD method onto the X40CrMoV5-1 hot work tool steel, HS6-5-2 high speed steel and SiAlON tool ceramics substrate.

2. Materials and methodology

The examinations were performed on specimens made of X40CrMoV5-1 hot work tool steel, HS6-5-2 high speed steel and SiAlON tool ceramics deposited in the PVD process with hard Ti(C,N), (Ti,Al)N and (Cr,Si,Al)N gradient coatings. To provide proper quality, steel specimens surfaces were proceeded by mechanical grinding and polishing (R_a=0, 03 µm). The process of coatings deposition was made with the use of a device based on the cathodic arc evaporation (CAE) method. Cathodes containing pure metals (Ti, Cr), the TiAl (50:50 at. %) alloy, and the AlSi (88:12 wt. %) alloy, were used for deposition of coatings. The base pressure was 5×10^{-6} mbar, the deposition temperature was approximately 350°C (in case of the Ti(C, N) coatings - 500°C). The deposition conditions are summarized in Table 1.

The film thickness was determined by kalotest technique. The craters 15mm in diameter were polished steel ball. This method's significance is the measurement of arising craters diameters. An average number of 5 craters were generated in each sample.

To obtain the coatings' microhardness, the Dynamic Ultra Microhardness Tester DUH 202 from Shimadzu Corporation was used. The Vickers indenter has 50 mN load, which provides that the penetration depth will not exceed 10% of coatings thickness. This eliminates the influence of substrate hardness on measurement result.

Observation of coatings structure and surface topography was carried out by use of ZEISS SUPRA 35 and OPTON DSM 940 scanning electron microscopes. To obtain the topography and fracture images the Secondary Electrons (SE) and Back Scattered Electrons (BSE) techniques were used with accelerating voltage of 15÷20 kV.

The structure and diffraction investigations of thin foils were performed on the JEOL 3010 transmission electron microscope at the accelerating voltage 300 kV. The electron diffraction from TEM was solved using an Eldyf computer application.

The roughness measurements of the substrate surface and samples with wear-resistant coatings were made with the use of laser scanning confocal microscope.

Phase composition analyses of studied samples were made by X-Ray Diffraction method on the DRON 2.0 device, using the filtered X-ray Kα tube with cobalt anode, at the voltage 40 kV and tube current 20mA.

Adhesions of deposited coatings to the substrate was examined by Scratch Test method, using CSEM Revetest device. Diamond indenter was shifted on surface coating with load increasing from 0 to 100 N, load increase rate (dL/dt) 100 N/min, indenter's speed (dx/dt) 10 mm/min. The critical load L_C was determined by acoustic emission level (AE) and observation of failure at the scratch.

The chemical concentration changes of the coating components, both perpendicular to their surface and in the transition zone between the coating and the substrate material were evaluated in virtue of tests carried out in the GDOS-750 QDP glow discharge optical spectrometer from Leco Instruments. The following operation conditions of the spectrometer Grimm lamp were met during the tests: lamp inner diameter– 4 mm; lamp supply voltage – 700 V; lamp current – 20 mA; working pressure – 100 Pa.

Table 1.
Deposition parameters of the coatings

Coating	Substrate bias voltage [V]	Arc current source [A]	Temperature [°C]	Gas mixture	
				Nitrogen flow rate [sccm]	Acetylene flow rate [sccm]
(Ti,Al)N	-60	TiAl – 60	350	100→250	–
(Al,Si,Cr)N	-60	Cr – 60 AlSi – 60	350	100→250	–
Ti(C,N)	-60	Ti – 60	500	250→100	0→200

3. Investigations results

X-ray diffraction patterns of investigated samples show that the coatings are composed of one Ti(C,N), (Ti,Al)N and (Cr,Si,Al)N fcc phase. It was found that X-ray spectra diffraction from Ti(C,N) coating onto SiAlON substrate contain TiN, TiC and Ti(C,N) phase peaks while the same type of coating onto both steels reveal Ti(C,N) phase peaks only (Fig. 1). In case of the (Cr,Si,Al)N phase the diffraction lines are shifted to lower diffraction angles as compared with the position of the lines for the CrN phases. This is due to an increase of the CrN elementary cell parameter with the NaCl structure as result of Cr atoms (r_{Cr} = 0.125 nm) substitution by Al atoms (r_{Al} = 0.143 nm). In all X-Ray diffraction pattern substrate peaks were present.

Fracture observations of the coatings by SEM (Figs. 2,3) show that (Ti,Al)N coating contains the columnar structure, which may be considered as compatible with the Thornton model (I zone) (Fig. 2a). Among larger, conical, narrowing to the pit crystals, there are smaller crystallites, which are filling the space between them. The other coatings structures are corresponding to IV zone (T) of the Thornton model. These coatings are characterized by compact fibrous structure without discontinuity and tight adherence to the substrate (Fig. 2b).

The coating observations in the TEM (Fig. 4, 5) indicate that such coatings consist of fine crystallites, of average size ca. 15-50 nm, depending on the kind of coating. Generally, there are no foundations to confirm the epitaxial growth of the investigated coatings.

Roughness of the studied samples, defined by R_a parameter was determined by laser scanning confocal microscope (Fig. 6a). Examinations have revealed the surface roughness increase resulting from deposition of PVD coatings (Table 2). In case of coatings deposited onto steels substrates, the greatest increase of R_a parameter is for Ti(C,N) coatings within the range of 0.19÷0.31 μm. Maximum increase of roughness parameter for SiAlON substrate reveal the (Ti, Al)N coating. The morphology of the coatings surfaces deposited on the substrate was characterized by a significant inhomogeneity due to numerous microdroplets (Fig. 3a, 6b) inherent to the used PVD coatings deposition process.

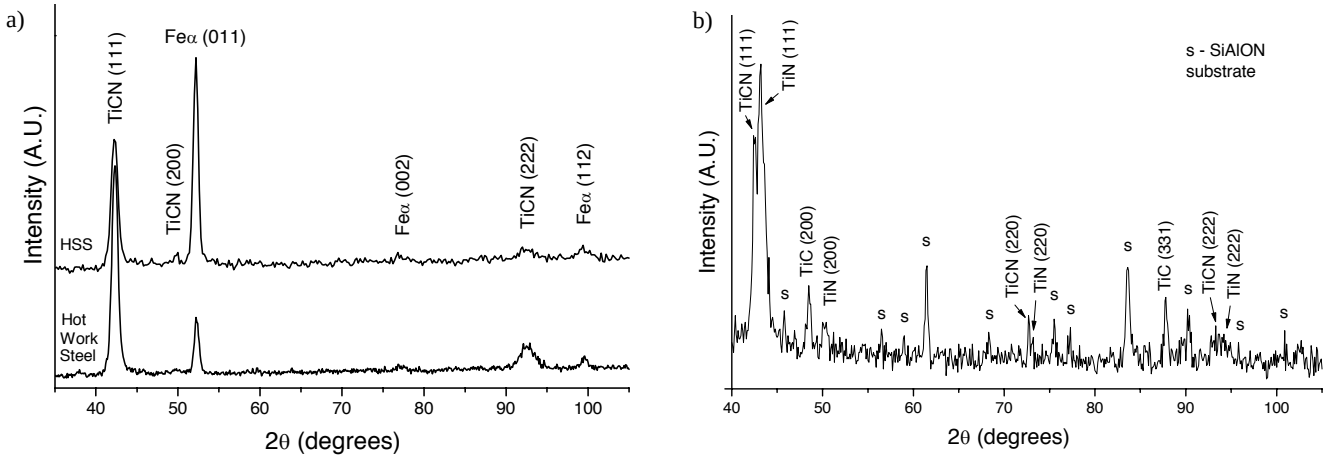

Fig. 1. X-ray diffraction pattern of Ti(C,N) coatings onto: a) high speed steel and hot work steel; b) SiAlON tool ceramics

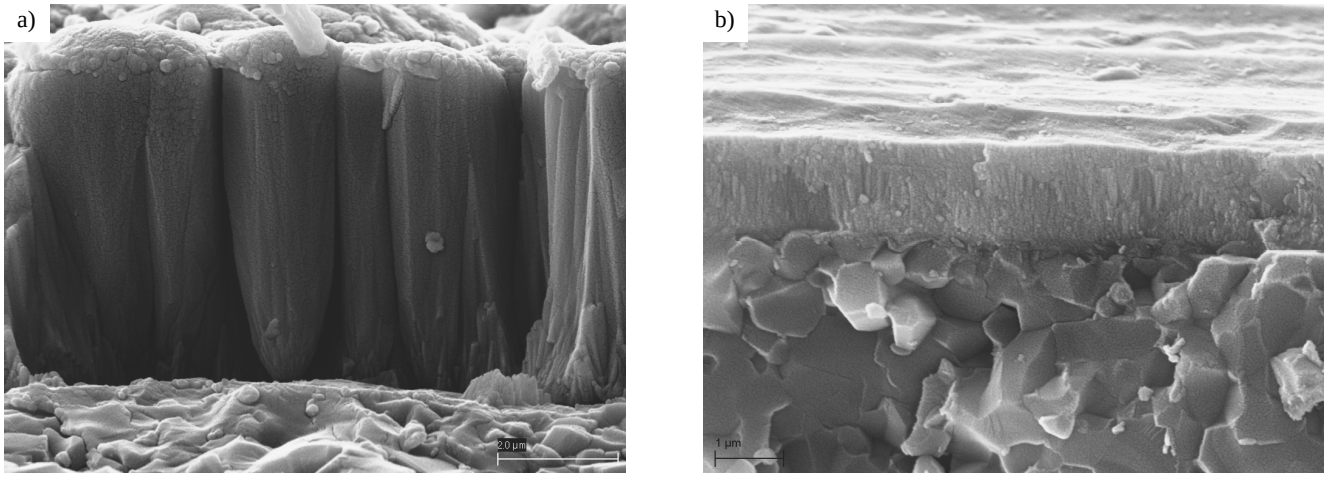

Fig. 2. Fracture of the coating deposited onto SiAlON substrate: a) (Ti, Al)N; b)Ti(C,N)

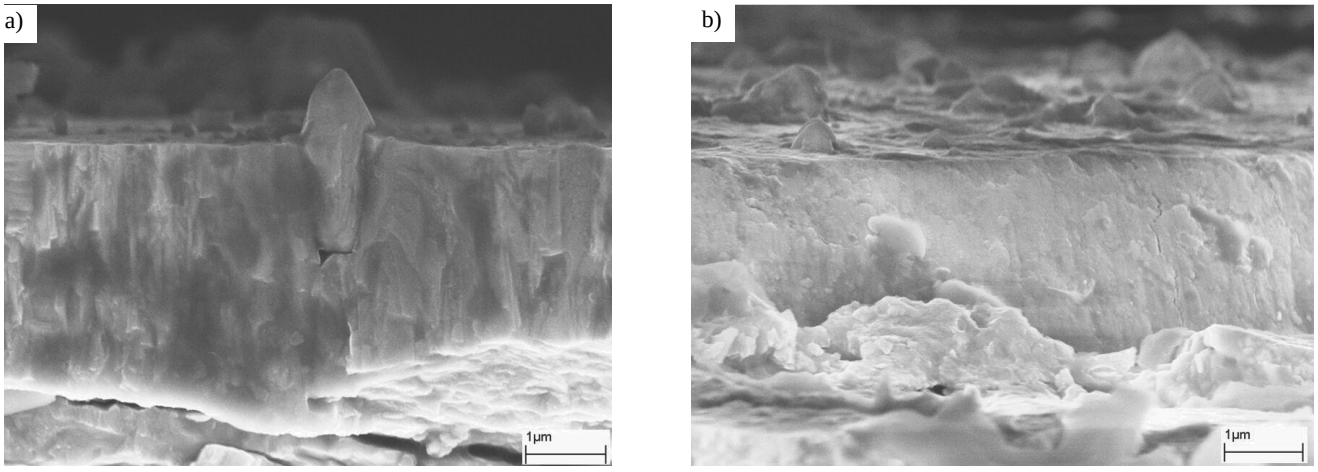

Fig. 3. Fracture of the coating deposited onto the X40CrMoV5-1 steel substrate: a) AlSiCrN, b) Ti(C,N)

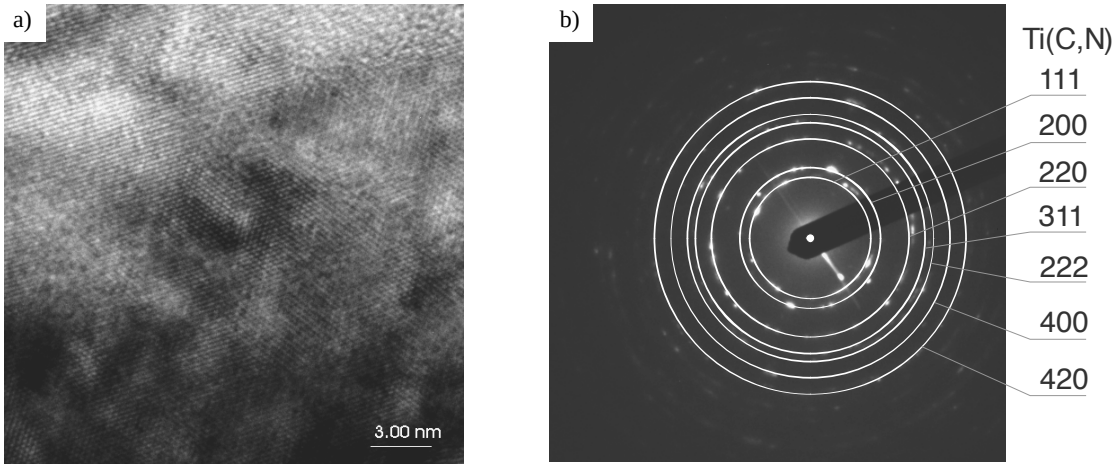

Fig. 4. a) Structure of the thin foil from the Ti(C,N) coating deposited onto the hot work tool steel X40CrMoV5-1, b) diffraction pattern from the area as in figure a and solution of the diffraction pattern

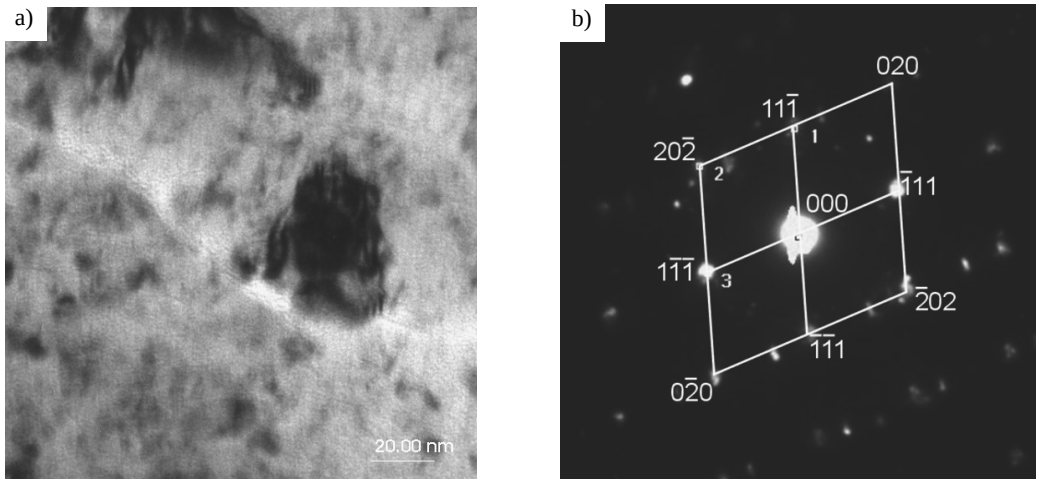

Fig. 5. a) Structure of the thin film of the AlSiCrN coating deposited onto the hot work tool steel X40CrMoV5-1, b) diffraction pattern from the area as in figure a and solution of the diffraction pattern indicating (Cr,Al)N phase

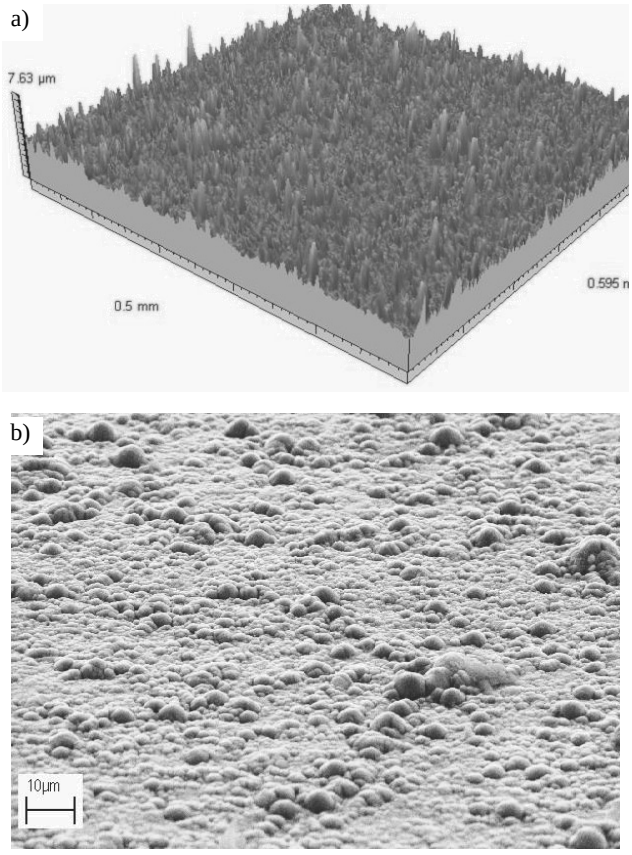

Fig. 6. Surface topography of (Ti,Al)N coating deposited on SiAlON tool ceramics substrate, a) laser scanning confocal microscope; b) scanning electron microscope

In the result of microhardness measurements for investigated uncoated samples and coated with PVD coatings, increased surface microhardness was found after coatings deposition (Table 2, Fig. 7).

Adhesion of examined coatings to substrates is characterized by the critical load L_{C1} and L_{C2}. These values were determined with the use of the scratch test with the linearly growing load. The friction force Ft and acoustic emission AE as a function of the load Fn during scratch testing were recorded (Figs. 9a, 10a, 11a). The critical load L_{C1} is a point on the curve of the friction force, where the first damage of the coating was observed and corresponding acoustics emission signal was recorded (Figs. 9b, 10b, 11b). L_{C2} is the second critical load, where the damage becomes continuous and complete delamination of the coating has been achieved (Figs. 9c, 10c, 11c). Scratch adhesion tracks were analyzed using the light microscope coupled with a measuring gauge. Thus the values of the critical load L_c could be obtained on the basis of metallographic observations.

The results of the scratch test measurement for the studied coatings are presented in Table 2 and in Figs. 8, 9a, 10a, 11a. They show that the greatest value of the first critical load L_{C1}=28 N is characteristic for Ti(C,N) coatings on hot work tool steel whereas the greatest value of the second critical load L_{C2}=90 N is characteristic for Ti(C,N) coatings on SiAlON tool ceramics. The lowest values of the critical loads are characteristic for (Cr, Si, Al) N coatings on all substrates. Moreover, the observations of scratch tracks confirmed the typical failure mode for this type of testing described by Burnett and Rickerby [15]. All coatings contain micro cracks, singular surface spallings outside or inside the tracks without any exposure of the material substrate. For higher loads, the other modes of failures occurred: cracking chipping, spallations and delamination outside and inside the track with the exposure of the material substrate to the highest load.

Table 2.
Specification of substrates and coatings investigated in the work

Substrate	Coating	Thickness, µm	Roughness, µm	Microhardness, HV	Critical load, N	
					L_{C1}	L_{C2}
High speed steel	uncoated	-	0.03	865 (66 HRC)	-	-
	Ti(C,N)	2.0	0.34	3100	23	67
	(Ti,Al)N	2.2	0.08	2800	25	49
	(Al,Si,Cr)N	1.8	0.21	3200	19	35
Hot work steel	uncoated	-	0.03	613 (56 HRC)	-	-
	Ti(C,N)	4.2	0.22	3000	28	59
	(Ti,Al)N	2.8	0.13	3300	19	46
	(Al,Si,Cr)N	2.1	0.20	3200	25	46
SiAlON	uncoated	-	0.12	2000	-	-
	Ti(C,N)	1.5	0.13	3200	17	90
	(Ti,Al)N	6.5	0.30	2900	18	77
	(Al,Si,Cr)N	1.2	0.23	2800	37	52

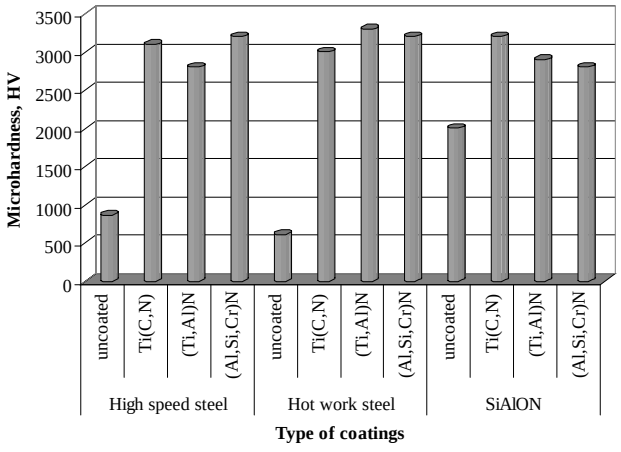

Fig. 7. Comparison of microhardness of investigated coatings deposited on different substrates

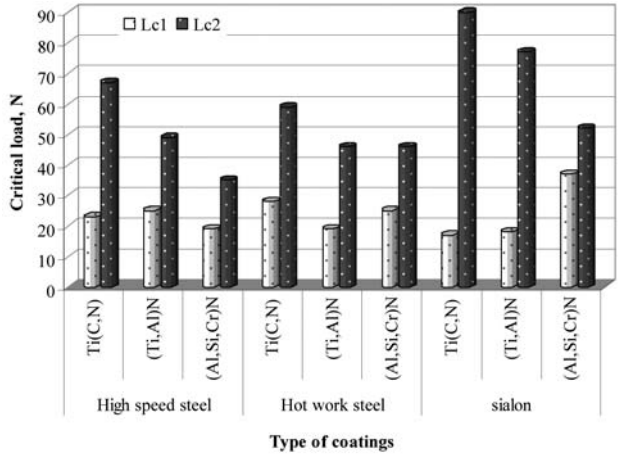

Fig. 8. Comparison of critical load of investigated coatings deposited on different substrates

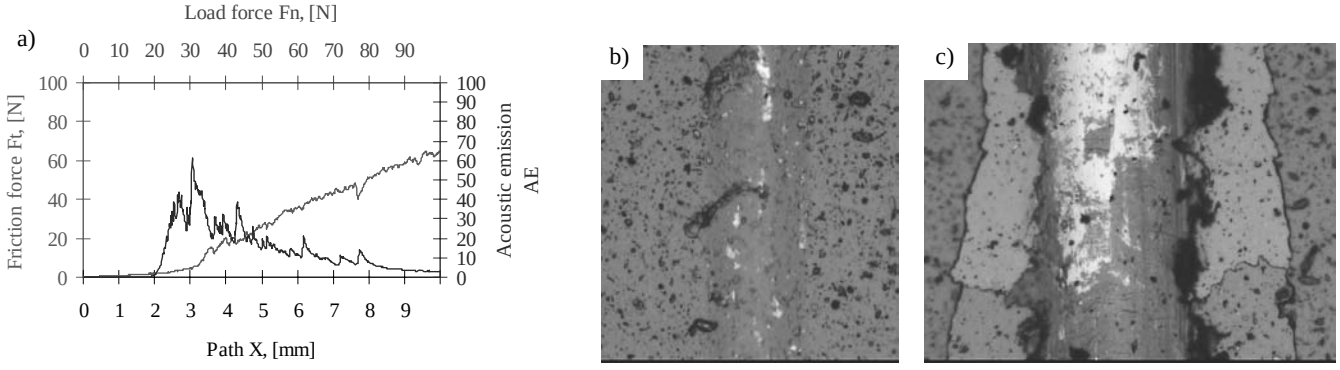

Fig. 9. Acoustic emission (AE) and friction force Ft as a function of the load Fn for (Cr,Si,Al)N gradient coating on HSS6-5-2 high speed steel and scratch failure at: b) L_{C1} 17N and c) L_{C2} 35 N

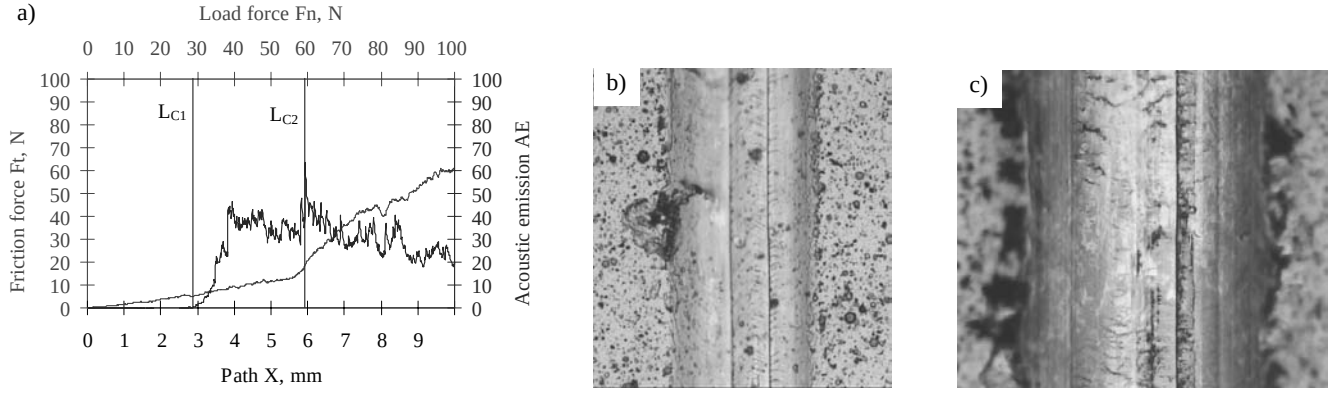

Fig. 10. Acoustic emission (AE) and friction force Ft as a function of the load Fn for Ti(C,N) gradient coating on X40CrMoV5-1 hot work tool steel and scratch failure at: b) L_{C1} and c) L_{C2}

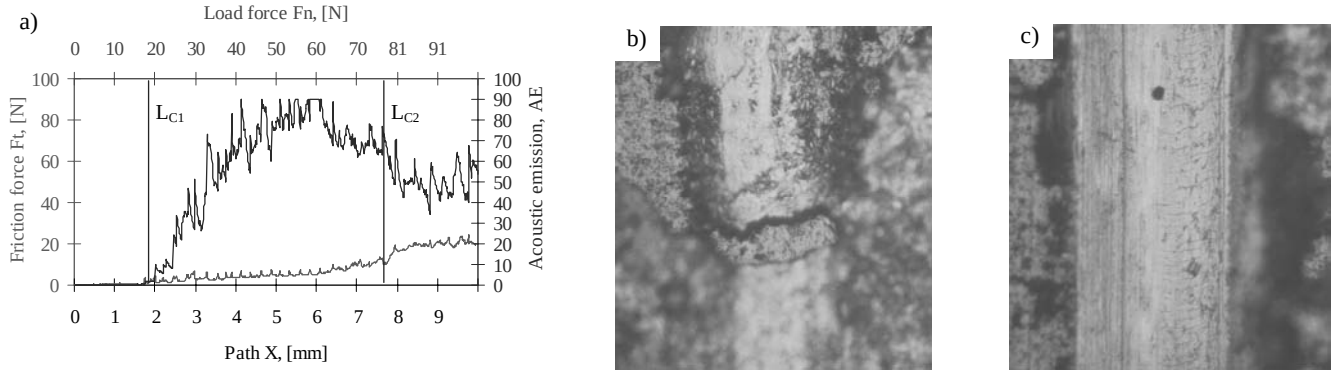

Fig. 11. Acoustic emission (AE) and friction force Ft as a function of the load Fn for (Ti,Al)N gradient coating on SiAlON tool ceramics and scratch failure at: b) L_{C1} and c) L_{C2}

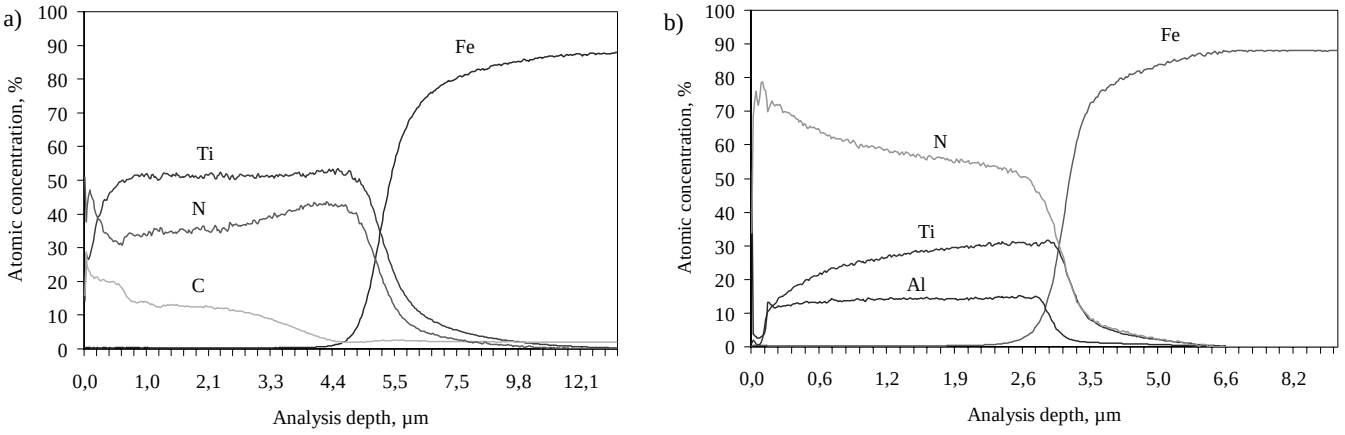

Fig. 12. Changes of constituent concentration of the coating and the substrate materials from coatings: a) Ti(C,N), b) (Ti,Al)

The GDOS tests also indicate the existence of the transition zone between substrate material and coating, improving adhesion of the deposited coatings to the substrate. In the transition zone the concentration of elements included in the substrate grows, while the concentration of elements constituting the coatings decreases rapidly. Its development may be also connected with high energy ions causing transfer of the elements in the joint zone, increase of desorption of the substrate surface, and development of defects in the substrate. It should be emphasised, however, that the results obtained with the use of the GDOS cannot be interpreted unequivocally, due to the inhomogeneous vaporisation of the specimen material during the tests. Fig. 12 present the changes of the chemical concentrations of the coating constituents and substrate material upon tests carried out on the glow-discharge optical emission spectroscope.

4. Summary

The compact structure of the coatings without any visible delamination was observed in the scanning electron microscope. The investigated coatings show columnar structure, which may be considered compatible with the Thornton model (zone I and IV). Upon examination of the thin films, it was found that the coatings were composed of fine crystallites. X-ray diffraction patterns of the investigated samples have shown that the coatings contain one fcc phase only.

The coating adhesion scratch tests disclose the cohesion and adhesion properties of the coatings tested. In virtue of the tests carried out, it was found that the critical load L_{C2} fitted within the range 46÷59 N for the coatings deposited on a substrate made of hot work tool steel X40CrMoV5-1, 35÷67 for the coatings deposited on a substrate of high speed steel HS6-5-2 and 52÷90 N for coatings deposited on the substrate made of the SiAlON. The coatings deposited on the substrate made of the SiAlON present a better adhesion than the coatings deposited on the substrate made of the tool steels. The highest value of the critical load was obtained for the Ti(C,N) coating. The GDOS investigations indicate the existence of the transition zone between the substrate material and the coating resulting in the improved adhesion of the coatings deposited to the substrate.

Acknowledgements

The paper has been realised in relation to the project POIG.01.01.01-00-023/08 entitled “Foresight of surface properties formation leading technologies of engineering materials and biomaterials” FORSURF, co-founded by the European Union from financial resources of European Regional Development Found and headed by Prof. L.A. Dobrzański.

References

[1] A.A. Voevodin, J.S. Zabinski, C. Muratore, Recent Advances in Hard, Tough, and Low Friction Nanocomposite Coatings, Tsinghua Science and Technology 10 (2005) 665-679.

[2] I. Dahan, U. Admon, N. Frage, J. Sariel, M.P. Dariel, J.J. Moore, The development of a functionally graded TiC-Timultilayer hard coatings, Surface and Coatings Technology 137 (2001) 111-115.

[3] U. Schulz, M. Peters, F.W. Bach, G. Tegeder, Graded coatings for thermal, wear and corrosion barriers, Materials Science and Engineering 362 (2003) 61-80.

[4] H. Jihua, L. Jinfeng, K. Akira, W. Ryuzo, A new method for fabrication of functionally gradient materials, Journal of Materials Science Letters 17 (1998) 2033-2035.

[5] L.A. Dobrzański, K. Gołombek, Structure and properties of the cutting tools made from cemented carbides and cermets with the TiN+mono-, gradient- or multi (Ti, Al, Si)N+TiN Nanocrystalline coatings, Journal of Materials Processing Technology 164-165 (2005) 805-815.

[6] L.A. Dobrzański, S. Skrzypek, D. Pakuła, J. Mikuła, A. Kriz, Influence of the PVD and CVD technologies on the residual macro-stresses and functional properties of the coated tool ceramics, Journal of Achievements in Materials and Manufacturing Engineering 35/2 (2009) 162-168.

[7] L.A. Dobrzański, K. Gołombek, J. Mikuła, D. Pakuła, Multilayer and gradient PVD coatings on the sintered tool materials, Journal of Achievements in Materials and Manufacturing Engineering 31/2 (2008) 170-190.

[8] L.A. Dobrzański, M. Staszuk, J. Konieczny, W. Kwaśny, M. Pawlyta, Structure of TiBN coatings deposited onto cemented carbides and sialon tool ceramics, Archives of Materials Science and Engineering 38/1 (2009) 48-54.

[9] L.A. Dobrzański, Engineering materials and materials design. Fundamentals of materials science and physical metallurgy, WNT, Warsaw-Gliwice, 2006 (in Polish).

[10] M. Kupczyk, Surface engineering. Wear resistant coatings for cutting edges, Poznan University of Technology Publishing House, Poznan, 2004 (in Polish).

[11] H. Mandal, New developments in α-SiAlON ceramics, Journal of the European Ceramic Society 19 (1999) 2349-2357.

[12] L. Chen, E. Kny, G. Groboth, Sialon ceramic with gradient microstructures, Surface Coating and Technology 100-101 (1998) 320-323.

[13] S. Kurama, The effects of processing on the α ↔ β SiAlON transformation during cycling heat treatments, Materials Science and Engineering 487/1-2 (2008) 278-288.

[14] B. Bitterlich, S. Bitsch, K. Friederich, SiAlON based ceramic cutting tools, Journal of the European Ceramic Society 28 5 (2008) 989-994.

[15] P.J. Burnett, D.S. Rickerby, The relationship between hardness and scratch adhesion, Thin Solid Films 154 (1987) 403-416.